Simulation Analyses of Seismic Tests of a Pile-Supported Structure in Liquefiable Sand Using Large-Scale Blast Excitation

Kontani Osamu [1], Tanaka Hideo [2], Ishida Tomoaki [2], Miyamoto Yuji [1] and Koyamada Kohji [1]

1) Kobori Research Complex Inc., 6-5-30, Akasaka, Minato-ku, Tokyo 107-8502 JAPAN
2) Power Engineering R&D Center, Tokyo Electric Power Co., 4-1 Egasaki, Tsurumi-ku, Yokohama 230-8510 JAPAN

ABSTRACT

Seismic tests have been conducted on a pile-supported structure in a liquefiable sand deposit using ground motions generated from large mining blasts. This paper presents simulation analyses of the seismic tests.

A 2-D finite element model (2-D FEM) was constructed and response analyses considering effective stresses were performed to simulate responses of the sand deposit and the adjacent free field. The analysis results confirmed that the effective stress analysis method could simulate the nonlinear behavior of a sand deposit under liquefaction.

A beam-interaction spring model was used to simulate the dynamic behavior of the pile-supported structure. The input motions to the beam-interaction spring model were obtained from the effective stress analyses using 2D-FEM. Comparison of the analysis results and the test results confirmed that the beam-interaction spring model employed here simulated the dynamic behaviors of the soil-pile-structure system very well.

INTRODUCTION

Seismic tests were conducted on a pile-supported structure in a liquefiable sand deposit using ground motions caused by large mining blasts at Black Thunder Mine, Wyoming, USA. The seismic tests and the investigation of test results are presented in the paper entitled "Seismic Tests of a Pile-Supported Structure in Liquefiable Sand Using Large-Scale Blast Excitation" [1] in this conference, SMiRT-16. This paper presents simulation analyses of seismic tests.

Table 1 summarizes the seismic tests. The tests were performed six times in total. The major advantages of carrying out seismic tests at a mining site are (1) large-scale test structure can be tested, (2) responses can be obtained at different levels for various levels of input motions, (3) soil-structure interaction and nonlinear behavior in three dimensions can be considered. As can be seen in Table 1, the maximum acceleration records at the ground surface of the adjacent free field vary from 20 Gals to 1353 Gals, which provides a wide variety of test results.

In this paper, the three tests highlighted in yellow in Table 1 were chosen for detailed investigation, because they provide three different phenomena in terms of liquefaction of the sand deposit. In Test-1, there was almost no liquefaction because of the small acceleration levels. In Test-5, the upper half to 2/3 of the test pit seemed to be liquefied based on the simulation analysis. In Test-3, the entire test pit was subject to liquefaction, which was recognized by simulation analysis results as well as test results. Sand boiling was observed in the test pit after seismic tests with larger input motions.

SIMULATION ANALYSIS OF TEST PIT AND FREE FIELD

2-D Finite Element Model

A 2-D FEM was constructed and used for simulation analyses of test results in the test pit and the adjacent free field. This is shown in Figure 1. In order to simulate strong nonlinear phenomena including liquefaction, nonlinear properties of sand and generation of pore water pressures were also considered in the response analyses [2]. A region 82m wide and 32m deep was modeled as 2-D FEM.

Table 1 Summary of Seismic Tests

Level of Input Motions	Test #	Distance * (m)	Maximum Acceleration **		
			EW	NS	UD
Small	Test-1	3000	20	28	29
	Test-2	1000	32	84	48
Medium	Test-5	500	142	245	304
Large	Test-3	140	579	568	1013
	Test-4	180	564	593	332
Very Large	Test-6	90	1217	1353	3475

*: distance from blast area to test site
**: at ground level of adjacent free field (Gals)

The properties of the soil layers were obtained from PS measurement at the test site, and are shown in Figure 1. The properties of the sand were determined from laboratory test results. Rayleigh damping was set at 5% for the first frequency (4.0Hz) of the soil layers. Fixed conditions and viscous conditions were applied to the bottom boundary and side boundaries, respectively, of the 2-D FEM. The acceleration records at 32m below ground level (GL-32m) were used as input motions to the 2-D FEM. In the response analyses, horizontal and vertical motions were simultaneously applied to the 2-D FEM.

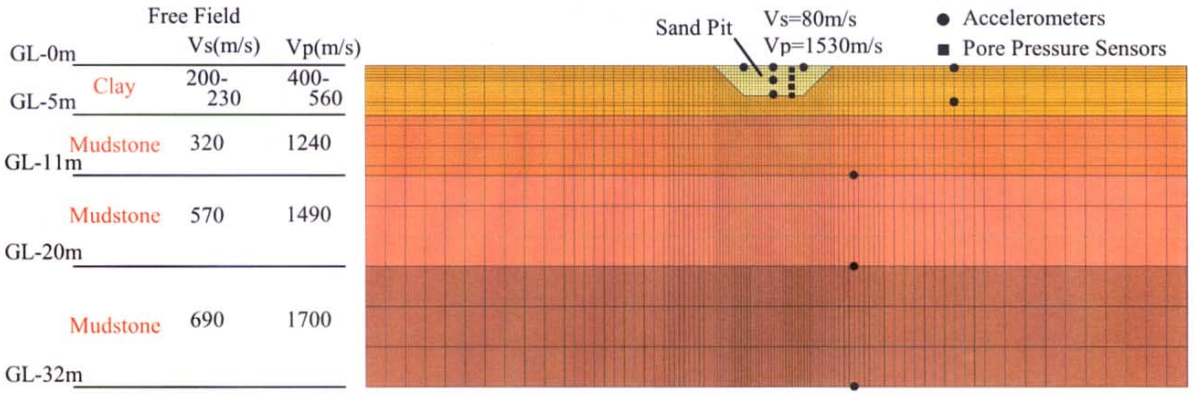

Figure 1 2-D Finite Element Model

Horizontal accelerations in the EW direction are discussed hereafter in this paper.

Results of Simulation Analysis

The distributions of the maximum acceleration obtained from the effective stress analysis are compared with the test results at the adjacent free field, as shown in Figure 2. The acceleration increased as ground motions traveled upward from GL-32m to the ground surface. This shows fair agreement between analysis results and test results, except for accerelation at the ground surface for Test-5. The reason for this small discrepancy seemed to be local alternation of the soil properties of the surface layer.

Figure 3 compares the maximum acceleration distributions from the mudstone layers through the sand obtainded from analysis results and test results. In the mudstone layers from GL-10m to GL-3m, there was very little amplification for all three tests. In the test pit, however, there were great differences in acceleration distributions because of the degree of liquefaction in the test pit. In Test-1 (Small Input Level), acceleration increased as the ground motions went upward. In Test-5 (Medium Input Level), there was a very little amplification throughout the depth of the test pit. In Test-3 (Large Input Level), the acceleration at the surface of the test pit was much less than the acceleration at the bottom of the test pit. In this case, shear waves could not propagate through the sand deposit becasue of liquefaction of the entire test pit.

Figure 4 compares the excess pore water pressures simulated by the effective stress analysis with test results for Test-3 (Large Input Level). As can be seen, there is good agreement between the analysis results and the test records. Even the fluctuations in pressure records due to longitudinal motions were simulated very well.

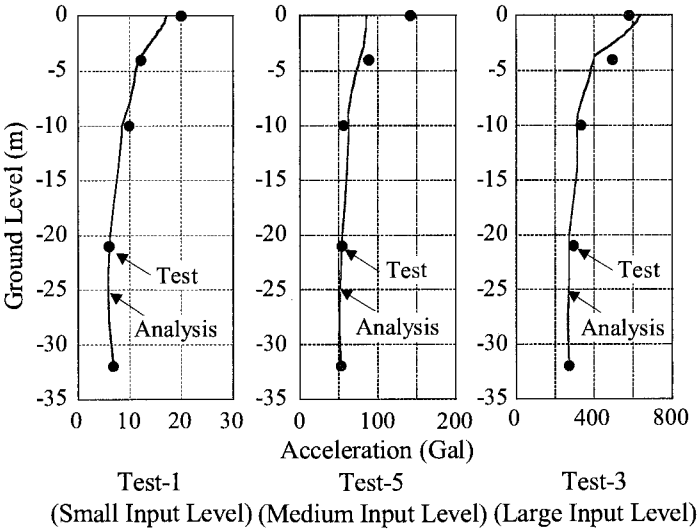

Figure 2 Maximum Acceleration at Free Field

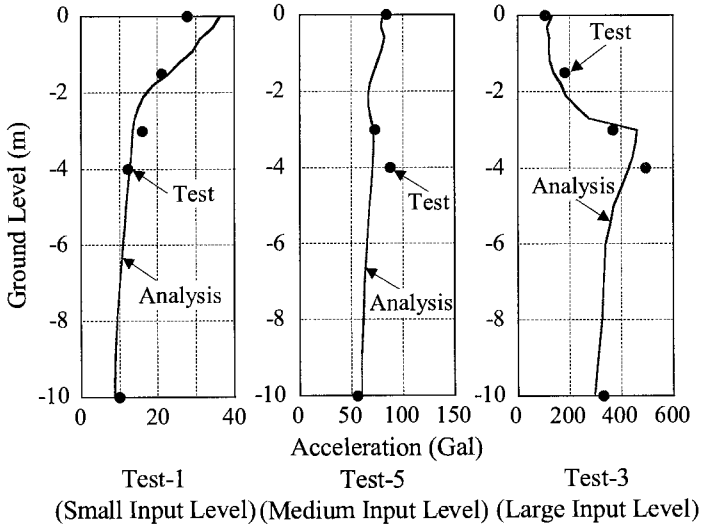

Figure 3 Maximum Acceleration at Test Pit

The ratio of excess pore water pressure to initial effective stress is a very common index for determining if liquefaction takes place in soil layers. The distributions of the ratios obtained from the effective stress analysis are shown in Figure 5.

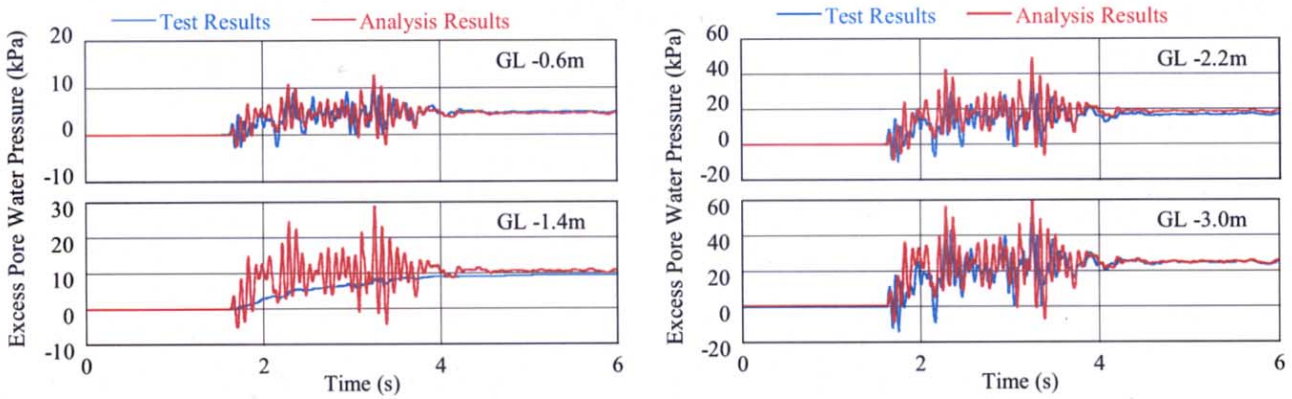

Figure 4 Simulation of Excess Pore Water Pressure (Test-3)

For Test-1 (Small Input Level), the entire section of the test pit is still blue and there seemed to be very little liquefaction. There are red areas at the upper edges of the section. Since there was a great differece between the sand deposit and surrounding mudstone layer in terms of shear wave velocity, there must be some concentration of vibration energy at the upper edge of the section. As a matter of fact, very small sand boiling phenomena were observed at the perimeter of the test pit surface.

For Test-5 (Medium Input Level), the analysis results indicated that a half to 2/3 of the pit depth seemed to be subject to liquefaction. This corresponds closely with the test results. The maximum excess pressures at GL-2.2m and at the bottom of the pit (GL-3.0m) were almost the same, and were less than the initial effective stresses.

For Test-3 (Large Input Level), analysis results indicated that the entire section of the test pit was subject to liquefaction. This can be seen from the excess pressure records of the test results.

Figure 6 compares the acceleration response spcetra evaluated by the response analyses with those from test records of Test-1 and Test-3. The response spectra in this figure are for the test pit surface and for the ground surface in the adjacent free field. The figure also shows the response spectra of the input motions to the 2-D FEM (acceleration records at GL-32m). During Test-1 (Small Input Level), the motion at GL-32m was amplified as they went upward to the surfaces of both the adjacent free field

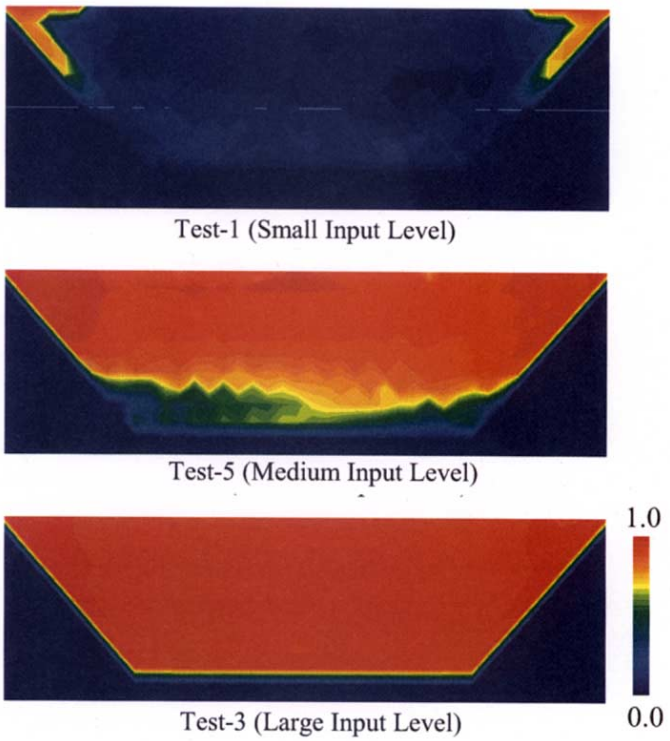

Figure 5 Distribution of Pore Water Pressure Ratio

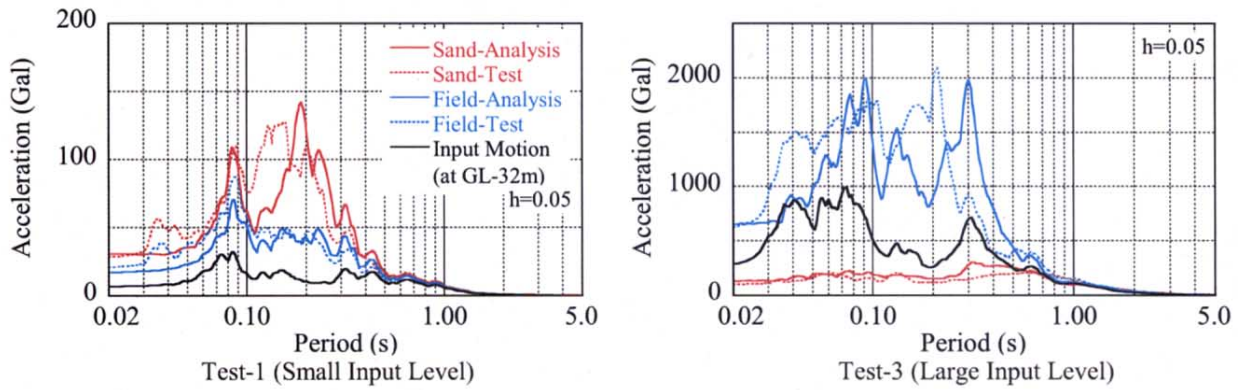

Figure 6 Acceleration Response Spectra at Ground Surface

and the test pit. Amplification was greater at the test pit than at the adjacent free field because soil layers in the free field were stiffer than the sand deposit. For Test-3 (Large Input Level), the motion at GL-32m was amplified as they traveled upward to the surface of the free field. Conversely, the response acceleration at the test pit surface was apparently smaller than that at GL-32m, because the test pit was subject to severe liquefaction during the seismic test.

Since the effective stress analysis simulated the test results very well, the same analysis method was employed to investigate the effects of longitudinal waves on the development of excess pore water pressures. Results regarding Test-3 are shown in Figure 7. The time histories shown in red were obtained from the response analyses with simultaneous horizontal and vertical input motions. Those shown in blue were obtained from the effective stress analysis with the horizontal input motion only. As can be seen very clearly, there were large effects of longitudinal motions in the course of the development of excess pore water pressures. However, the longitudinal motions did not seem to have an important role in the liquefaction, since very little effect was found on residual pore water pressure values.

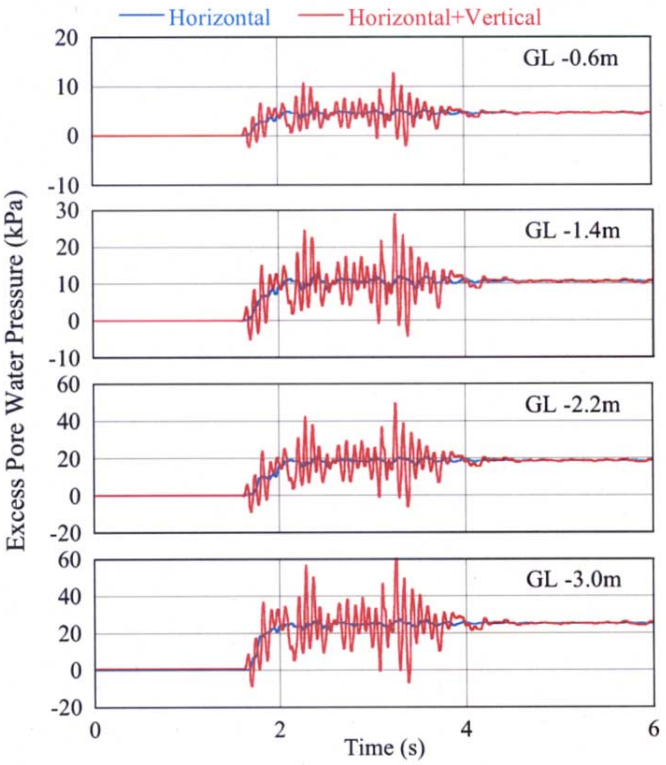

Figure 7 Effects of Longitudinal Wave Motions on Excess Pore Water Pressure Development Test-3 (Large Input Level)

SIMULATION ANALYSIS OF PILES AND STRUCTURE

Numerical Model for Dynamic Response Analysis

A dynamic response analysis using a beam-interaction spring model [3][4] was performed to simulate the test results of the piles and the structure. The model is shown in Figure 8. The pile foundation was modeled by a one-stick model with lumped masses and beam elements. The lumped masses were connected to soil layers in the free field through nonlinear lateral interaction springs modified step by step in accordance with the developed excess pore water pressures. The dynamic response analyses of the soil-pile-structure system are conducted with inputs of time histories of soil displacements and excess pore water pressures at each level obtained from response analyses of the test pit using 2-D FEM.

The initial values of lateral and shear interaction soil springs needed to be evaluated in accordance with the linear properties of soil layers [4][5]. The relationships between lateral loads and displacements for four piles were strictly obtained using Green's functions with ring loads in the layered stratum [6]. The rotational spring was modeled and evaluated at the pile head level. The axial stiffness of the piles and the bearing capacities of the supporting mudstone layer were incorporated into the evaluation. No friction between piles and surrounding sand was taken into

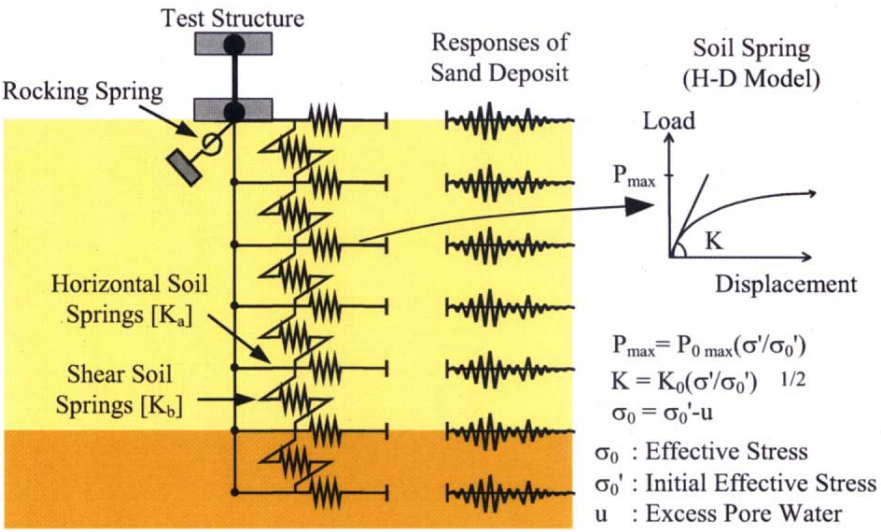

Figure 8 Beam-Interaction Spring Model of Soil-Pile-Structure System

account. The damping coefficients of the springs were determined on the basis of the first natural frequency of the soil-pile-structure interaction system.

The structure was simply modeled as two masses and one beam element. The stiffnesses of steel columns and piles were obtained from mill sheets. Damping factors of 1% were used for both reinforced concrete and steel columns.

Results of Dynamic Response Analysis

Figure 9 compares the distributions of the maximum pile bending moments obtained from the response analyses with those evaluated from strain measurement records of one pile in the tests. There is very good agreement between analysis results and test results. The maximum bending moment occurred at the pile head regardless of input motion levels. However, the distribution shapes varied in accordance with input motion levels.

The bending moment generated on the piles by earthquake motions can be divided into two moment components based on the mechanism causing it, as described in Figure 10. One component is caused by inertial forces from the structure on the pile foundation. The other is caused by soil displacements due to ground motions. In this paper, the moment caused by earthquake motions is called "total moment", and the former and the latter components are called "inertial component" and "kinematic component", respectively. The kinematic component can be obtained from response analyses using the numerical model of soil-pile-structure system shown in Figure 8. In this case, however, a mass-less structure is used to evaluate the effects only from soil displacements. The inertial components are obtained by subtracting kinematic components from total moments in the time domain.

In order to investigate the effects of inertial forces and soil displacements on bending moment generation, the total moments evaluated from the response analyses were divided into inertial components and kinematic components, as shown in Figure 11. The inertial components took their maximum values at the pile heads and the kinematic components showed larger values at the pile heads and at the interface between the sand and mudstone layers at GL-3m, regardless of input motion level. As input motion levels increased, the inflection point of the total moment moved down from GL-1.3m to GL-2.2m. It was found that different total moment distribution shapes were determined mainly by inertial components, and that the influence of inertial force on total moment increased as input motion levels increasd, because the surrounding sand lost its stiffness due to severe liquefaction.

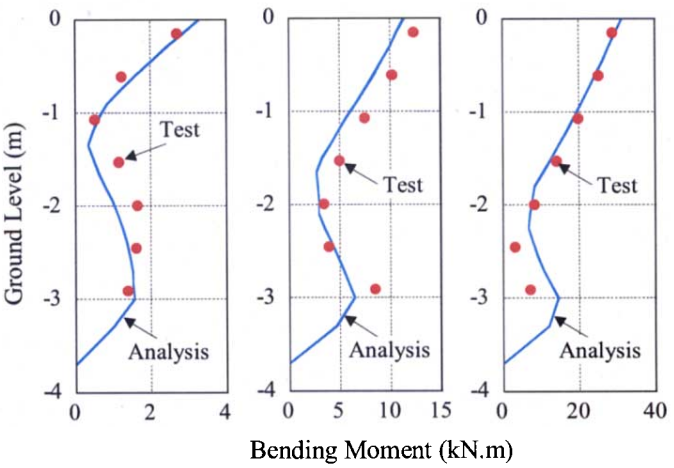

Test-1 (Small Input Level) Test-5 (Medium Input Level) Test-3 (Large Input Level)

Figure 9 Distribution of Maximum Bending Moment

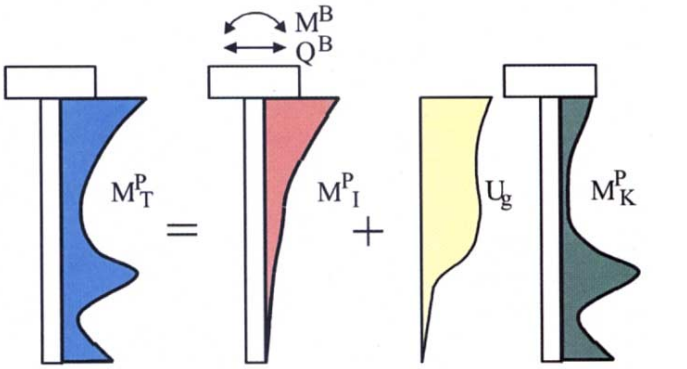

Total Moment | Inertial Component caused by Structure | Kinematic Component caused by Soil Displacements

Figure 10 Mechanism of Bending Moment Generation

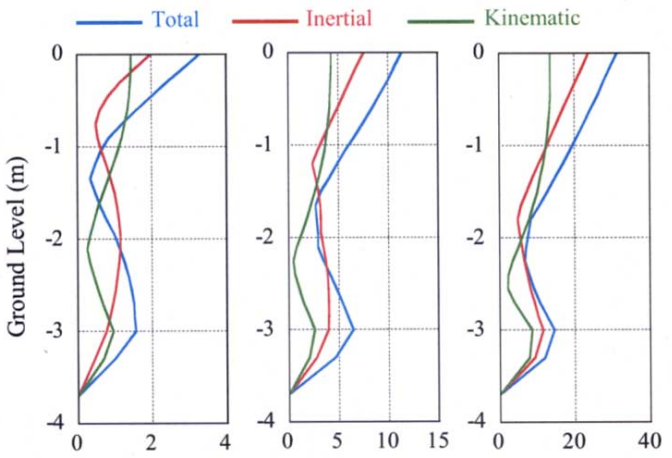

Test-1 (Small Input Level) Test-5 (Medium Input Level) Test-3 (Large Input Level)

Figure 11 Moment Component caused by Inertial Forces and Soil Displacements

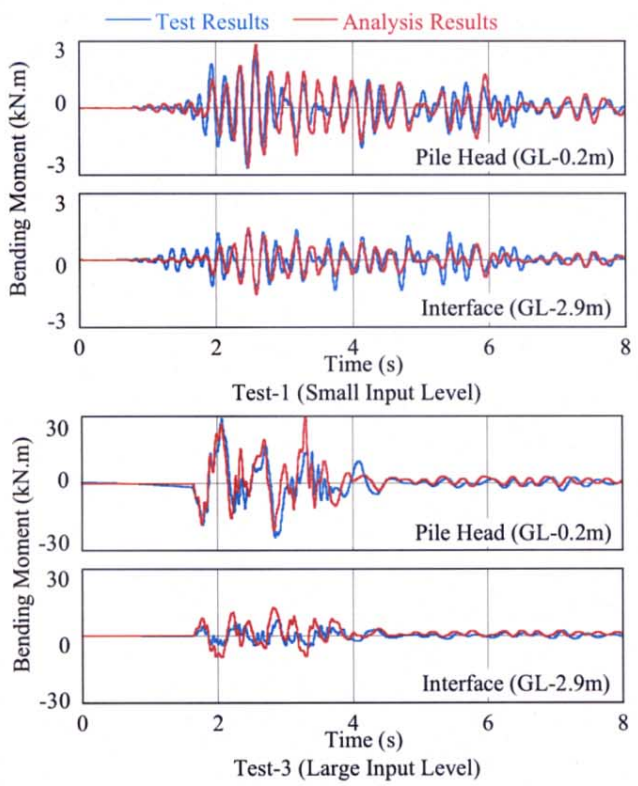

Figure 12 Comparison of Pile Bending Moment

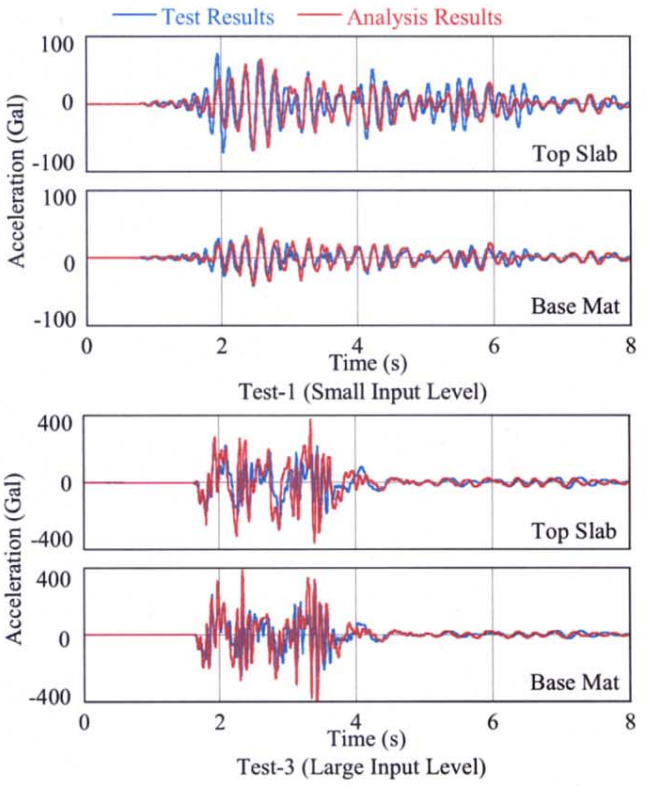

Figure 13 Comparison of Test Structure Response

Figure 12 compares the time histories of the bending moments evaluated from the response analyses with those obtained from the test results. The moments in this figure were evaluated at the pile heads and at the interface between the sand and the mudstone layers. Although the timing of the maximum moments was different, there is very good agreement between the shapes of the wave forms.

Figure 13 compares the time histories of the acceleration evaluated from response analyses with those obtained from the test results. The acceleration in this figure was evaluated at the top slab and the base mat. There is a very good agreement between the time histories for Test-1. Although the maximum acceleration obtained from the analysis results was a little greater than that from test results, the overall tendencies of the test results of the soil-pile-structure system were expressed by the analysis very well for Test-3.

Figure 14 compares the response spectra obtained from response analyses with those from test results. The response spectra at the top slab and at the base mat are shown in this figure. For Test-1, the responses at the top slab were larger than those at the base mat over the entire period. For Test-3, the responses at the top slab were larger than those at the base mat, except for periods longer than 0.1 seconds. There was some discrepancy between the response acceleration levels for Test-3. However, the analysis results simulated the tendency of the test results very well.

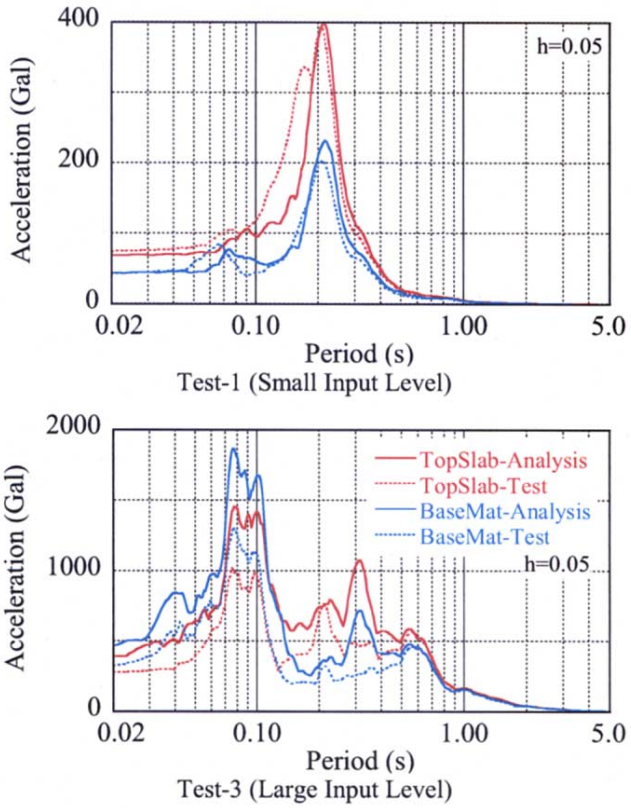

Figure 14 Comparison of Test Structure Response

Response Analysis Methods for Evaluating Pile Bending Moment

The dynamic and static analysis methods using the beam-interaction spring model are commonly employed for evaluating pile bending moment during earthquake. The models used are shown in Figure 15. In order to investigate if these analysis methods can evaluate pile bending moment during earthquake, the dynamic and static response analyses were conducted and analysis results were compared with test results.

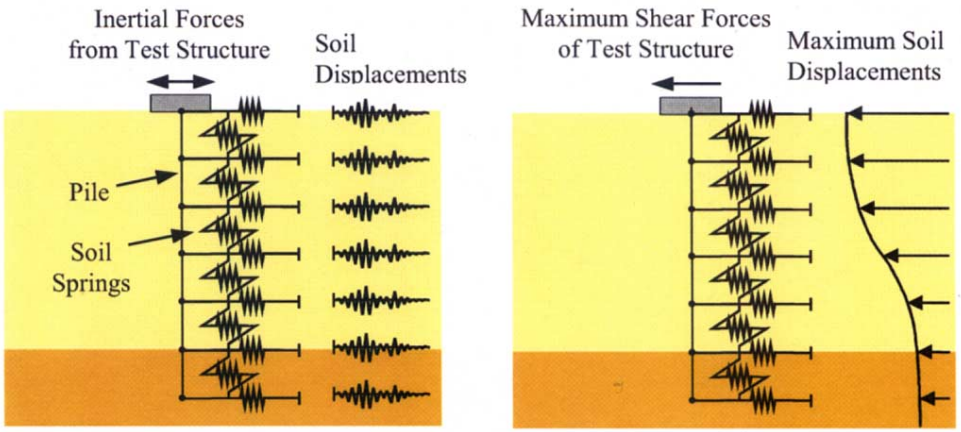

Dynamic Analysis Model Static Analysis Model

Figure 15 Models for Response Analysis

The input motions for the dynamic method are evaluated from separate analyses. The soil displacements were obtained from the effective stress analysis using 2-D FEM, and the inertial forces were evaluated from the test results at the base mat.

In the static analysis method, the maximum soil displacements at each level were applied to piles through soil springs, and the maximum shear forces from the structure were applied to the pile head. The maximum displacement was obtained from effective stress analyses using 2-D FEM at each level. The maximum shear forces correspond to the maximum values of inertial force time histories that were used in the dynamic analysis as input motions.

Figure 16 compares the bending moments of the piles obtained from two analysis methods with the evaluated test results. For Test-1 (Small Input Level), the dynamic and static analysis methods provided almost the same results. Both showed smaller moments than the test results at around GL-2.0m. For Test-5 (Medium Input Level), the dynamic analysis method provided results that were closer to the test results than the static analysis method.

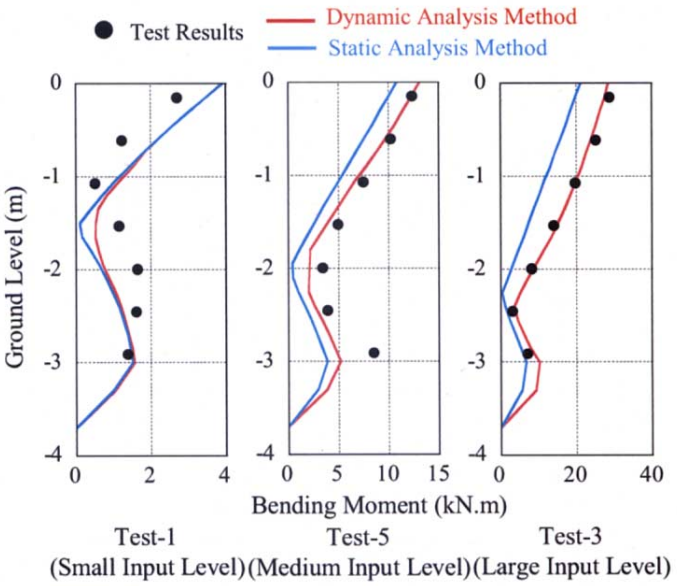

Figure 16 Comparison of Pile Bending Moment Obtained by Dynamic and Static Analysis Methods

For Test-3 (Large Input Level), the dynamic analysis method provided analysis results that were very close to the test results. Conversely, the static analysis method underestimated the test results, because the soil springs were evaluated on the basis of complete liquefaction. If the static response analysis method is employed for the situation as in Test-3, great care needs to be taken in evaluating nonlinear properties of soil springs and maximum response displacements.

CONCLUSIONS

Dynamic Response Analysis of Test pit and Adjacent Free Field

1) It was confirmed that the dynamic effective stress analysis using 2-D FEM could simulate the dynamic behavior of a sand deposit from linear conditions to nonlinear conditions including liquefaction very well.
2) The acceleration at the surface of the sand deposit was greater than in an adjacent free field when the input motions were relatively small. As the levels of input motions increased, the acceleration at the surface of the sand deposit became much smaller than in an adjacent free field due to liquefaction.
3) Numerical analyses have confirmed that the excess pore water pressure was greatly influenced by longitudinal waves in the course of developing excess pressure, and that longitudinal waves had very little influence on residual excess pore water pressure values.

Response Analysis of Piles and Structure

1) It was confirmed that a dynamic response analysis using a beam-interaction spring model could simulate the behaviors of piles and the structure during liquefaction very well. This method can be used to accurately evaluate the bending moment of piles and the responses of the structure during liquefaction.
2) When the static response analysis method is employed to evaluate the bending moment of piles, it is very important to evaluate the nonlinear properties of the soil springs.
3) The bending moment showed its maximum value at the pile heads and a large value at the interface between the sand deposit and the mudstone layer. As input motion levels increased, the inflection point of the total moments moved downward and the proportion of inertial component in the total bending moment became greater than that of kinematic component because the surrounding sand lost its stiffness

ACKNOWLEDGMENTS

We would like to express our deep appreciation to Dr. Aoyama, Professor Emeritus of University of Tokyo, for his guidance throughout this experimental research. We would also like to thank Dr. Miura, Professor of University of Hiroshima, for his review of the experimental results and the analysis results.

The project staff from OYO International, Agbabian Associates, GeoVision, and CE&MT are also thanked for their dedicated assistance with the field studies.

Most importantly, we would like to thank the management and staff of Arch Coal's Black Thunder Mine for their assistance throughout the project. Special thanks go to Paul Lang, to Steve Beil and to the late Bob Martin. They were always very generous and provided us with support in many ways. Without their help, this work would not have been possible.

REFFERENCE

1. Kamijho, N., Saito, H., Kusama, K., Kontani, O. and Nigbor, R., "Seismic Tests of a Pile-Supported Structure in Liquefiable Sand Using Large-Scale Blast Excitation," *Proceeding of the 16th International Conference on Structural Mechanics in Reactor Technology* (SMiRT-16), 2001, Washington
2. Iai, S., Matsunaga, Y. and Kameoka, T., "Strain Space Plasticity Model for Cyclic Mobility," *Soils and Foundation*, Vol.32, No.2, 1992, pp.1-15
3. Miyamoto, Y., Miura, K., Scott, R. F. and Hushmand, B., "Pile Foundation Response in Liquefiable Soil Deposit during Strong Earthquake," *Journal of Structural and Construction Engineering*, Architectural Institute of Japan, No. 439, 1992 (in Japanese)
4. Miyamoto, Y., Sako, Y., Kitamura, E. and Miura, K., "Earthquake Response of Pile Foundation in Nonlinear Liquefiable Sand Deposit," *Journal of Structural and Construction Engineering*, Architectural Institute of Japan, No. 471, 1995, pp.41-50 (in Japanese)
5. Miyamoto, Y., Fukuoka, A., Adachi, N. and Koyamada, K., "Pile Response induced by Inertial and Kinematic Interaction in Liquefiable Deposit - Centrifuge Model Test for Pile Foundation in Saturated Sand Layers and its Analytical Study," *Journal of Structural and Construction Engineering*, Architectural Institute of Japan, No. 494, 1998, pp.51-58 (in Japanese)
6. Kausel E. and Peek R., "Dynamic Loads in the Interior of a Layered Stratum- An Explicit Solution", *Bulletin of the Seismological Society of America*, Vol. 72, 1982, pp. 1459-1481